

ROSAT PSPC observations of T Tauri stars in MBM12*

T. Hearty¹, R. Neuhauser¹, B. Stelzer¹, M. Fernández¹, J.M. Alcalá², E. Covino², and V. Hambaryan³

¹ Max-Planck-Inst. für Extraterrestrische Physik, D-85740 Garching, Germany

² Osservatorio Astronomico di Capodimonte, I-80131 Napoli, Italy

³ Astrophysikalisches Institut Potsdam, An der Sternwarte 16, D-14482, Potsdam, Germany

Received 25 May, 1999; accepted 22 October, 1999

Abstract. We present the *ROSAT* PSPC pointed and *ROSAT* All-Sky Survey (RASS) observations and the results of our low and high spectral resolution optical follow-up observations of the T Tauri stars (TTS) and X-ray selected T Tauri star candidates in the region of the high galactic latitude dark cloud MBM12 (L1453-L1454, L1457, L1458). Previous observations have revealed 3 “classical” T Tauri stars and 1 “weak-line” T Tauri star along the line of sight to the cloud. Because of the proximity of the cloud to the sun, all of the previously known TTS along this line of sight were detected in the 25 ks *ROSAT* PSPC pointed observation of the cloud. We conducted follow-up optical spectroscopy at the 2.2-meter telescope at Calar Alto to look for signatures of youth in additional X-ray selected T Tauri star candidates. These observations allowed us to confirm the existence of 4 additional TTS associated with the cloud and at least 2 young main sequence stars that are not associated with the cloud and place an upper limit on the age of the TTS in MBM12 \sim 10 Myr.

The distance to MBM12 has been revised from the previous estimate of 65 ± 5 pc to 65 ± 35 pc based on results of the *Hipparcos* satellite. At this distance MBM12 is the nearest known molecular cloud to the sun with recent star formation. We estimate a star-formation efficiency for the cloud of 2–24%.

We have also identified a reddened G9 star behind the cloud with $A_v \sim 8.4$ –8.9 mag. Therefore, there are at least two lines of sight through the cloud that show larger extinctions ($A_v > 5$ mag) than previously thought for this cloud. This higher extinction explains why MBM12 is capable of star-formation while most other high-latitude clouds are not.

Key words: Stars:formation – ISM:clouds

1. Introduction

The nearest molecular cloud complex to the sun (distance ~ 65 pc) consists of clouds 11, 12, and 13 from the catalog of Magnani et al. (1985) and is located at (l,b) \sim (159.4, -34.3). This complex of clouds (which we will refer to as MBM12) was first identified by Lynds (1962) and appears as objects L1453-L1454, L1457, L1458 in her catalog of dark nebulae. The mass of the entire complex is estimated to be ~ 30 –200 M_\odot based on radio maps of the region in ^{12}CO , ^{13}CO and C^{18}O (Pound et al. 1990; Zimmermann & Ungerechts 1990).

Recently, there has been much interest in understanding the origin of many isolated T Tauri stars (TTS) and isolated regions of star-formation. For example, within ~ 100 pc from the sun there are at least two additional regions of recent star-formation: the TW Hydrae association (distance ~ 50 pc; e.g. Kastner et al. 1997; Webb et al. 1999) and the η Chamaeleontis region (distance ~ 97 pc; Mamajek et al. 1999). Both of these star-forming regions appear to be isolated in that they do not appear to be associated with any molecular gas. In addition, both are comprised mainly of “weak-line” TTS¹. In contrast, most of the TTS in MBM12 are CTTS which are still associated with their parent molecular cloud.

In addition to the above isolated star-forming regions, TTS have been found outside of the central cloud core regions in many nearby star-forming cloud complexes (see references in Feigelson 1996). Several theories exist to explain how TTS can separate from their parent molecular clouds either by dynamical interactions (Sterzik & Durisen 1995) or by high-velocity cloud impacts (Lépine & Duvert 1994). Feigelson (1996) also suggests that some of these TTS may form in small turbulent cloudlets that dissipate after forming a few TTS. Since the TTS in MBM12 appear to still be in the cloud in which they formed, we know they have not been ejected from some other more distant star-forming region. Therefore

¹ We define “weak-line” TTS (WTTS) to be TTS with $H\alpha$ equivalent widths, $W(H\alpha) > -10\text{\AA}$ and “classical” TTS (CTTS) to be TTS with $W(H\alpha) < -10\text{\AA}$ where the negative sign denotes emission

Send offprint requests to: thearty@xray.mpe.mpg.de

* Table 4 is only available in electronic form at the CDS via anonymous ftp to cdsarc.u-strasbg.fr (130.79.128.5) or via <http://cdsweb.u-strasbg.fr/Abstract.html>.

MBM12 may be an example of one of the cloudlets proposed by Feigelson (1996). Moriarity-Schieven et al. (1997) argue that MBM12 has recently been compressed by a shock associated with its interface with the Local Bubble. This shock may also have recently triggered the star-formation currently observed in MBM12 (cf. Elmegreen 1993). Alternatively Ballesteros-Paredes et al. (1999) suggest that MBM12 may be an example of a star-forming molecular cloud that formed via large scale streams in the interstellar medium.

MBM12 is different from most other high-latitude clouds at $|b| > 30^\circ$ in terms of its higher extinction and its star formation capability (e.g., Hearty et al. 1999). Based on CO observations and star counts, the peak extinction in the cloud is $A_V \sim 5$ mag (Duerr & Craine 1982a; Magnani et al. 1985; Pound et al. 1990; Zimmermann & Ungerechts 1990). However, molecular clouds are clumpy and it is possible that some small dense cores with $A_V > 5$ mag were not resolved in previous molecular line and extinction surveys. For example, Zuckerman et al. (1992) estimate $A_V \sim 11.5$ mag through the cloud, along the line of sight to the eclipsing cataclysmic variable H0253+193 located behind the cloud and we estimate $A_V \sim 8.4$ – 8.9 along the line of sight to a G9 star located on the far side of the cloud (Sect. 4)

Although there is evidence for gravitationally bound cores in MBM12, the entire cloud does not seem to be bound by gravity or pressure (Pound et al. 1990; Zimmermann & Ungerechts 1990). Therefore, the cloud is likely a short-lived, transient, object similar to other high latitude clouds which have estimated lifetimes of a few million years based on the sound crossing time of the clouds (Magnani et al. 1985). If this is the case, MBM12 will dissipate in a few million years and leave behind an association similar to the TW Hydrae association that does not appear to be associated with any molecular material.

Previous searches for TTS in MBM12 have made use of H α , infrared, and X-ray observations. The previously known TTS in MBM12 are listed in Table 1 with their coordinates, spectral types, apparent magnitudes, and selected references. We include the star S18 in the list even though Downes & Keyes (1988) point out that it could be an Me star rather than a T Tauri star since our observations confirm that it is a CTTS. The previously known and new TTS stars identified in this study are plotted in Fig. 1 with an IRAS 100 μ m contour that shows the extent of the cloud.

Although the TTS LkH α 264 is a well studied object because of its extreme CTTS features (i.e., strong H α emission and infrared excess) and it is known to have strong Li I λ 6708 Å absorption (Herbig 1977), there is no measurement for the equivalent width of the lithium line, W(Li), of this star in the literature. The only previously known T Tauri star in this cloud which has a published measurement of W(Li) is E02553+2018 which was first identified as a T Tauri star in the *Einstein* Extended

Table 1. Previously known T Tauri stars in MBM12

Star	RA [2000]	Dec [2000]	SpT	V [mag]	Ref.
LkH α 262	2:56:07.9	20:03:25	M0	14.6	1,2
LkH α 263	2:56:08.4	20:03:39	M4	14.6	1,2
LkH α 264	2:56:37.5	20:05:38	K5	12.5	1,2,3,4
E02553+2018	2:58:11.2	20:30:04	K4	10:	2,5
S18	3:02:20.0	17:10:35	M3	13.5	6,7

(1) Herbig & Bell (1988). (2) Fernández et al. (1995). (3) Magnani et al. (1995). (4) Gameiro et al. (1993). (5) Caillault et al. (1995). (6) Stephenson (1986). (7) Downes & Keyes (1988) point out this could be an Me star rather than a T Tauri star.

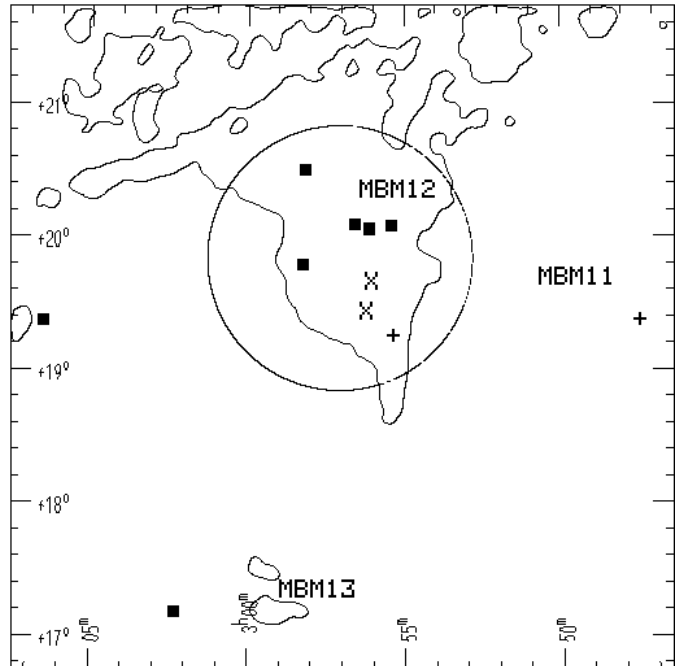


Fig. 1. The contour shows the extent of the IRAS 100 μ m emission from MBM12 in the region where we investigated the RASS data. The circle shows the region observed in the *ROSAT* PSPC pointed observation. The squares mark the locations of the 8 TTS in MBM12. The two stars LkH α 262 and LkH α 263 are separated by $\sim 15''$ and thus not resolved in this figure. The plus symbols mark the locations of two young *ROSAT* detected main sequence stars which still contain lithium, and the crosses mark the two lines of sight through the cloud which are known to have $A_V > 5$ mag. This and all subsequent figures use J2000 coordinates.

Medium Sensitivity Survey (EEMSS) (Gioia et al. 1990; Stocke et al. 1991). More recently, Martín et al. (1994) presented a high resolution spectrum of this star for which they measured $W[\text{Li}] = 475$ mÅ. Caillault et al. (1995) reported an X-ray count rate for this source of 0.008 counts s^{-1} in the *Einstein* band. None of the other TTS in the cloud have been previously detected in X-rays.

We present the *Hipparcos* satellite observations in Sect. 2 that show the distance to MBM12 is not as well constrained as previously thought and our high resolution observations of two TTS in the cloud that indicate the TTS are probably at the same distance as the cloud. In Sect. 3 we describe the *ROSAT* All-Sky Survey (RASS) and *ROSAT* pointed observations investigated. In Sect. 4 we present the results of our low-resolution spectroscopic observations of the T Tauri star candidates. In Sect. 5 we discuss the X-ray variability of the TTS and in Sect. 6 we derive an X-ray luminosity function for the TTS in MBM12. In Sect. 7 we present our conclusions.

2. The distance to MBM12 and its T Tauri stars

2.1. The distance to the gas

The distance to MBM12 was first estimated by Duerr & Craine (1982a) using Wolff diagrams. They found evidence for two clouds along this line of sight: one cloud at a distance of 200–300 pc with a typical visual extinction of $\sim 2\text{--}3$ mag and another cloud at a distance of 500–800 pc with a typical visual extinction of ~ 1.5 mag. However, more recent observations show that this is probably one complex of molecular gas at a much smaller distance.

A more accurate estimate of the distance was reported by Hobbs et al. (1986) and Hobbs et al. (1988). The method used was to identify 10 bright stars in the direction of the cloud for which a *spectroscopic* parallax could be determined and look for interstellar Na I D lines in the spectra of these stars. They found that the star HD18404 (distance ~ 60 pc) showed no interstellar absorption features and is therefore presumably in front of the cloud and the star HD18519/20 (distance ~ 70 pc) did show interstellar absorption features and is therefore behind the cloud. Since observations of the other 8 stars are consistent with these two stars, most investigators have assumed a distance of $\sim 65 \pm 5$ pc for the cloud.

Since the *Hipparcos* satellite measured the *trigonometric* parallax of most of these stars it is no longer necessary to assume a spectral type or intrinsic luminosity (as is necessary for a spectroscopic parallax) to measure their distance. According to *Hipparcos*, the distance to HD18404 is $\sim 32 \pm 1$ pc and the distance to HD18519/20 is $\sim 90 \pm 12$ pc. The stars used by Hobbs et al. (1986) and Hobbs et al. (1988) to establish the distance to MBM12 are listed in Table 2 along with their apparent magnitude, spectral type, distance based on spectroscopic parallax, distance based on the *Hipparcos* parallax, and whether the spectrum presented in Hobbs et al. (1986) and Hobbs et al. (1988) showed interstellar Na I absorption lines. Although the *Hipparcos* results indicate the distance to MBM12 is not as well constrained as thought, it is consistent with the previous result (i.e., $\sim 65 \pm 35$ pc). However, since the revised distance estimate has $\sim 50\%$ uncertainty it cannot be used to derive accurate parameters for the TTS in the cloud.

Table 2. Stars from Hobbs et al. (1986) and Hobbs et al. (1988)

HD	HIP	V [mag]	SpT	Distance [pc]		NaI
				spectroscopic	<i>Hipparcos</i>	
18090	...	8.85	F3V	145	...	yes
18091	13579	7.00	A9V	85	96 ± 11	no
18190	...	8.98	A9V	185	...	yes
18256	13702	5.63	F6V	25	35 ± 1	no
18283	13723	8.78	A8III	380	150 ± 29	yes
18404	13834	5.80	F5IV	60	32 ± 1	no
18484	13892	6.70	A3III	211	141 ± 35	yes
18508	13913	7.34	F2V	80	91 ± 8	no
18519/20	13914	4.63	A2V	70	90 ± 12	yes
18654	14021	6.79	A0V	160	128 ± 18	yes

Zimmermann & Ungerechts (1990) point out that, although the distance estimate based on the two bright stars from Hobbs et al. (1986) and Hobbs et al. (1988) is valid for the northern section of the cloud, radio observations of the molecular gas show there are at least 4 velocity components that may all be at different distances. However, the polarization map of MBM12 produced by Bhatt & Jain (1992) shows that the polarization of the stars in the upper region of the cloud (where the Hobbs et al. 1986 and Hobbs et al. 1988 stars are located) is the same as that of the lower region of the cloud. Thus, they argue that the entire complex is at the same distance.

Zimmermann & Ungerechts (1990) also find that the ratio of the CO mass to the virial mass $M(\text{CO})/M_{\text{vir}} = 0.03$ for the whole cloud indicating the entire cloud is not gravitationally bound. However, they point out that some of the cores in the larger clumps may be gravitationally bound. If the cloud is found to be at a somewhat greater distance, these results will support the hypothesis that a few of the large clumps are gravitationally bound.

2.2. The association of the stars with the gas

Although the TTS and the cloud are projected along the same line of sight, they may be at different locations and thus not associated with each other. However, we can check whether the radial velocities of the stars are similar with the gas to find out if it is likely that the T Tauri stars are associated with the cloud. The distribution of cloud velocities are quite large with at least 4 components with average velocities -5.0 km s^{-1} (I), -2.3 km s^{-1} (II), 1.4 km s^{-1} (III), and 5.0 km s^{-1} (IV) (Zimmermann & Ungerechts 1990; Pound et al. 1990; Moriarty-Schieven et al. 1997).

We obtained high resolution spectra of two of the T Tauri stars in MBM12 with FOCES at the Calar Alto 2.2-m telescope in August 1998. The spectra for these stars (RXJ0255.4+2005 and LkH α 264, see Fig. 3.) allow us to estimate their radial velocities and confirm the W(Li) measurements of our low resolution spectra presented in

Table 3. Radial Velocities of the TTS in MBM12

Star	V_{lsr} [km s ⁻¹]	$v \sin i$ [km s ⁻¹]
RXJ0255.4+2005	4.5 ± 1.0	10.0 ± 3.0
LkH α 264 ^a	-4.2 ± 2.5	24.3 ± 2.0

^a Herbig (1977) measured a radial velocity of $\sim 1.0 \pm 3.9$ km s⁻¹ for this object.

Sect. 4. Determinations of radial velocity, RV, and projected rotational velocity, $v \sin i$, have been obtained by means of cross correlation analysis of the stellar spectra with those of radial velocity and rotational standard stars, treated in analogous way. Given the large spectral range covered by the FOCES spectra, the cross correlation of the target and template stars was performed after rebinning the spectra to a logarithmic wavelength scale, in order to eliminate the dependence of Doppler shift on the wavelength. Moreover, only parts of the spectra free of emission lines and/or not affected by telluric absorption lines have been used. Therefore, the NaI D, and H α lines as well as wavelengths longer than about 7000 Å have been excluded from the cross-correlation analysis. The result of the cross-correlation is a correlation peak which can be fitted with a Gaussian curve. The parameters of the Gaussian, center position and full-width at half-maximum (FWHM) are directly related to RV and $v \sin i$, respectively. The method of the correlation has been fully described by Queloz (1994), and Soderblom et al. (1989). More details about the calibration procedure can be found in Appendix A of Covino et al. (1997).

The radial velocities we measured for the two MBM12 TTS listed in Table 3 are similar to that of the molecular gas (Zimmermann & Ungerechts 1990; Pound et al. 1990). Radial velocity measurements have not yet been made for the fainter stars. Nevertheless, the superposition of the TTS on the cloud and the similar radial velocities of at least two of the stars with the gas are strong evidence to support that the TTS are associated with the cloud.

3. The *ROSAT* observations of MBM12

Since both CTTS and WTTS are typically $\sim 10^3$ – 10^5 times more luminous in the X-ray region of the spectrum than average (i.e., older) low-mass stars (Damiani et al. 1995), we made use of the *ROSAT* pointed and the RASS observations of MBM12 to identify previously unknown TTS in the cloud. The 25 ks *ROSAT* PSPC pointed observation (Sequence number 900138) was centered at (RA,Dec) \sim (2:57:04.8,+19:50:24). Although they were originally discovered by other means, all of the previously known TTS in the central region of MBM12 were also detected with *ROSAT*. Since the extent of the molecular gas is not known (in particular for the MBM13 region) and TTS can sometimes be displaced several parsecs from their parent clouds, we also searched in the RASS

database in a ~ 25 deg² region around MBM12. Details about *ROSAT* and its PSPC detector can be found in Trümper (1983) and Briel & Pfeffermann (1995), respectively. The RASS broad-band image of the region investigated around MBM12 and the *ROSAT* pointed observations are displayed in Fig. 2.

The X-ray source search was conducted in different *ROSAT* standard “bands”, defined as follows: “broad” = 0.08–2.0 keV; “soft” = 0.08–0.4 keV; “hard” = 0.5–2.0 keV; “hard1” = 0.5–0.9 keV; “hard2” = 0.9–2.0 keV. We identified all of the X-ray sources above a maximum likelihood² threshold of 7.4 in both the RASS and the *ROSAT* PSPC pointed observations of MBM12. In addition, we selected only those X-ray sources above a count rate threshold of ~ 0.03 cts s⁻¹ in the RASS observation and a count rate threshold of 0.0013 cts s⁻¹ in the *ROSAT* PSPC pointed observation. The one previously known TTS candidate, S18, near the cloud MBM13 was detected in the RASS with a ML = 6.4 (i.e., below our threshold), however, since our optical spectroscopic observations confirm that it is a TTS we include it in our study. We identified 49 X-ray sources in the *ROSAT* PSPC pointed observation of MBM12 (including all of the previously known TTS in the central region of the cloud) and 28 X-ray sources detected in the RASS (including S18) in the regions displayed in Fig. 2. Three stars were detected both on the RASS and in the pointed observation.

We list the sources detected in the *ROSAT* PSPC pointed observation and in the RASS in Table 4. We include the *ROSAT* source name, the X-ray source coordinates, the maximum likelihood for existence for each source, the broad-band count rates, the X-ray hardness ratios *HR1* and *HR2* (as defined in Neuhäuser et al. 1995), the apparent visual magnitude taken from the Guide Star Catalog (magnitudes for the fainter sources indicated with a “:” are estimated from the digitized sky survey images), and the broad-band X-ray to optical flux ratio. We also list the spectral type and the H α and lithium equivalent widths of the sources that have been observed spectroscopically and comments collected from our search through the SIMBAD³ and NED⁴ databases concerning the objects.

Assuming a mean X-ray count-rate-to-flux conversion factor of 1.1×10^{-11} erg cts⁻¹ cm⁻², which we derive from X-ray spectral fits of the TTS in Sect. 6, if the cloud is at a distance of 65 pc, the limiting luminosities of the observations are 1.7×10^{29} erg s⁻¹ and 7.2×10^{27} erg s⁻¹ for the RASS and *ROSAT* pointed observations, respectively. Therefore, these observations are sufficient to detect most of the WTTS in the cloud since the threshold is below the

² The maximum likelihood can be converted into probability P through the equation $P = 1 - \exp(-\text{ML})$.

³ This research has made use of the SIMBAD database, operated at CDS, Strasbourg, France.

⁴ The NASA/IPAC Extragalactic Database (NED) is operated by the Jet Propulsion Laboratory, Caltech, under contract with the National Aeronautics and Space Administration.

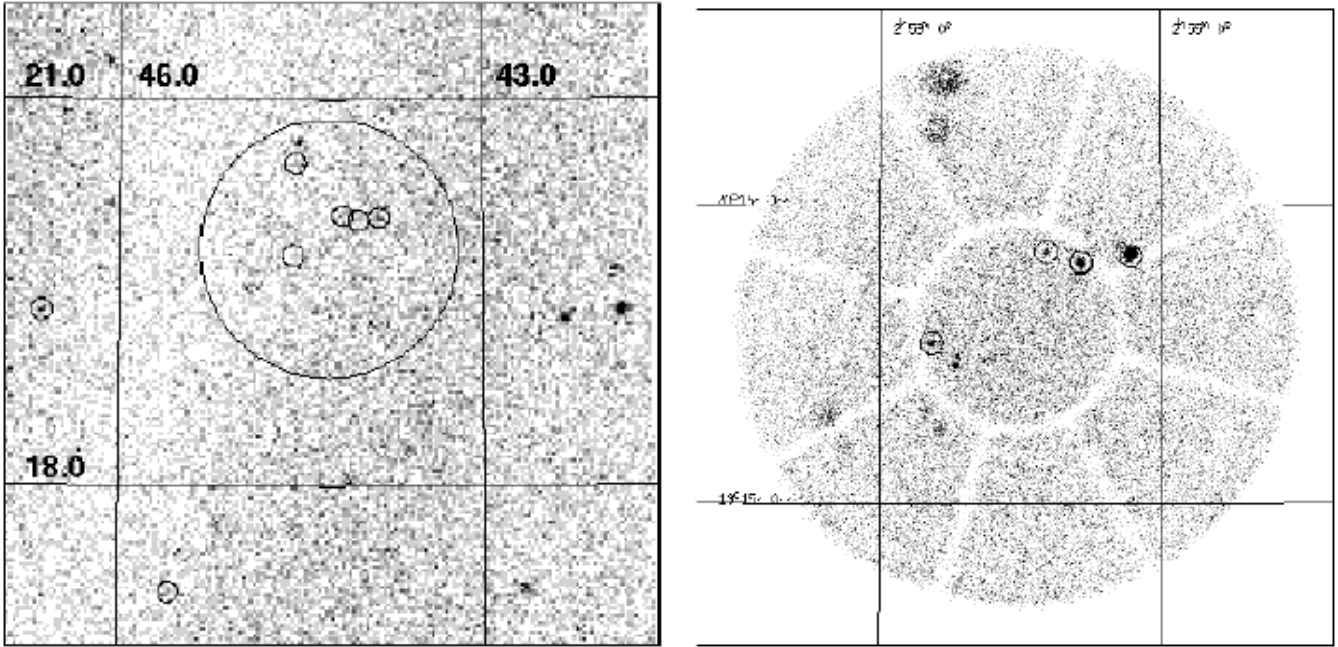


Fig. 2. A RASS broad-band (0.08–2.0 keV) image of the region we investigated around MBM12 is displayed in the left frame. The large circle showing the field of view of the pointed observation which is displayed in the right frame. The small circles mark the locations of the X-ray identified TTS in MBM12. The mean RASS exposure time in this region of the sky is quite low ~ 340 s, therefore only 3 of the TTS in this region were above our detection threshold and one, S18, was slightly below our threshold. However all of the TTS in the field of view of the pointed observation were clearly detected.

X-ray faintest stars in the WTTS X-ray luminosity function (e.g., Neuhäuser et al. 1995). Although the RASS observation of MBM12 is not sensitive enough to detect all of the CTTS in the cloud, the objective prism survey by Stephenson (1986) identified all of the $H\alpha$ emission sources in this region down to a visual magnitude threshold of ~ 13.5 . Since this limiting magnitude corresponds to the early M spectral types in MBM12, the current population of TTS in MBM12 presented in this paper should be complete for all earlier spectral types.

Since MBM12 is at relatively high galactic latitude, many of the 81 X-ray sources we identified are extragalactic. Therefore, we used the X-ray to optical flux ratios (see Table 4) to remove extragalactic sources from our list of candidates (cf. Hearty et al. 1999). All sources which have $\log(f_x/f_v) > 0.0$ are considered to be extragalactic and those with $\log(f_x/f_v) < 0.0$ are considered to be stellar objects, some of which could be PMS. We also searched the literature to remove cataloged non-PMS stars from our list of candidates. Finally we were left with a list of X-ray sources identified in the RASS and *ROSAT* pointed observations of the cloud which have stellar optical counterparts that may be PMS stars. However, many of these stars may be other types of X-ray active stars (e.g., RS CVn and dMe stars) and nearby main sequence stars (which may not be intrinsically X-ray bright, but are near enough so that their X-ray flux is large) that are more difficult to separate

from PMS stars by X-ray observations alone. Therefore, follow-up spectral observations are necessary to identify which X-ray sources are T Tauri stars.

4. The optical spectroscopy

In order to complete the census of the TTS population of MBM12 we require follow-up observations. Since lithium is burned quickly in convective stars, a measurement of $W(\text{Li})$ along with a knowledge of the spectral type of a star can be a reliable indicator of youth. Therefore we obtained broad-band, low-resolution, optical spectra of the X-ray emitting TTS candidates to determine spectral types and measure the equivalent width of the $H\alpha$ emission and Li I 6708 Å absorption lines.

The spectra were obtained from October 9–11, 1998 with the Calar Alto Faint Object Spectrograph (CAFOS) at the 2.2-m telescope at Calar Alto, Spain. The $24\mu\text{m}$ pixels of the SITE-1d 2048 \times 2048 chip with the G-100 grism provided a reciprocal dispersion of ~ 2.1 Å pixel $^{-1}$. The resolving power, $R = \lambda/\delta\lambda \sim 1000$, derived from the measurement of the FWHM (FWHM ~ 6.4 Å) of several well isolated emission lines of the comparison spectra is sufficient to resolve the lithium absorption line in T Tauri stars. The wavelength range ~ 4900 to 7800 Å was chosen to detect two indicators of possible youth ($H\alpha$ emission and Li I $\lambda 6708$ Å absorption) and to de-

termine spectral types. All spectra were given an initial inspection at the telescope. If a particular star showed signs of youth or the integration produced fewer than ~ 1000 cts pixel $^{-1}$, at least one additional integration was performed. The results of the spectroscopic observations of the TTS in MBM12 are summarized in Table 5. We list the name of the star; the coordinates for the optical source; the spectral type; the log of the effective temperature, $\log T_{\text{eff}}$, assuming luminosity class V and using the spectral type-effective temperature relation of de Jager & Nieuwenhuijzen (1987); apparent magnitude, V , taken from the Guide Star Catalog⁵; the equivalent width of H α , $W(\text{H}\alpha)$; both the low and high resolution (when available) measurements of $W(\text{Li})$; the veiling corrected $W(\text{Li})$ (cf. Strom et al. 1989); and the derived lithium abundance based on the non-LTE curves of growth of Pavlenko & Magazzù (1996) assuming $\log g=4.5$. The estimated error for the low-resolution $W(\text{Li})$ measurements is $\sim \pm 90$ mÅ based on the correlation with the three stars for which we have high resolution measurements.

The optical spectra of the TTS in MBM12 are displayed in Fig. 3. The stars which show strong H α emission are also scaled by an appropriate factor to display the emission line. The spectra of the two stars we classify as young main sequence stars which still show lithium are displayed in Fig. 4.

In addition to confirming that the star S18 is a CTTS with strong H α emission and Li I absorption, we identified 3 previously unknown TTS in MBM12. In order to estimate the relative age of the MBM12 stars with lithium we plot them in an $W(\text{Li})$ vs. T_{eff} diagram (Fig. 5) along with stars from Taurus (age \sim a few Myr), the TW Hydrae Association (age \sim 10 Myr), the η Chamaeleontis Cluster (age \sim 2–18 Myr), IC 2602 (age \sim 30 Myr), and the Pleiades (age \sim 100 Myr). In addition, we plot isoabundance lines for the non-LTE curves of growth of Pavlenko & Magazzù (1996) for $\log g=4.5$ stars and the isochrones for the non-rotating lithium depletion model of Pinsonneault et al. (1990). The positions of the MBM12 stars in the diagram indicates they are young objects with ages much less than that of the Pleiades or IC 2602. Although the relative ages between the stars in MBM12, the TW Hydrae Association, and the η Chamaeleontis Cluster, cannot be discerned in Fig. 5, since most of the TTS in MBM12 are CTTS which are still associated with their parent molecular cloud the TTS in MBM12 must be younger than those in the TW Hydrae Association or the η Chamaeleontis Cluster which are comprised mainly of WTTS not associated with any molecular cloud (i.e., the TTS in MBM12 have ages < 10 Myr).

Although the two F and G spectral type stars in which we detected lithium (HD 17332 and RXJ0255.3+1915) are located above the Pleiades in the $W(\text{Li})$ vs. T_{eff} diagram,

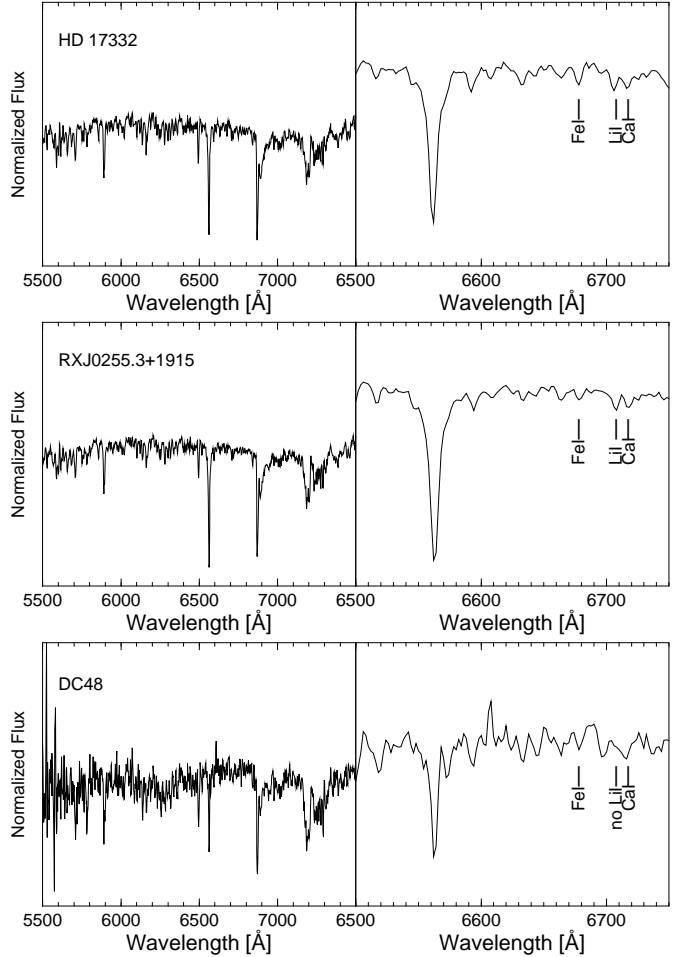


Fig. 4. Spectra of the young main sequence stars, HD 17332 and RXJ0255.3+1915, which have not yet depleted their lithium are displayed. We also show the spectrum of the highly reddened ($A_v \sim 8.4$ – 8.9) G9 star, DC48, which is located behind MBM12.

since they both show H α absorption stronger than any similar spectral type stars in IC 2602 (e.g., Randich et al. 1997), they are probably older than 30 Myr. Thus, we list them as main sequence stars in Table 5. Covino et al. (1997) have shown that low-resolution spectra tend to overestimate $W(\text{Li})$ in intermediate spectral types, therefore we probably over estimated the $W(\text{Li})$ for these two stars.

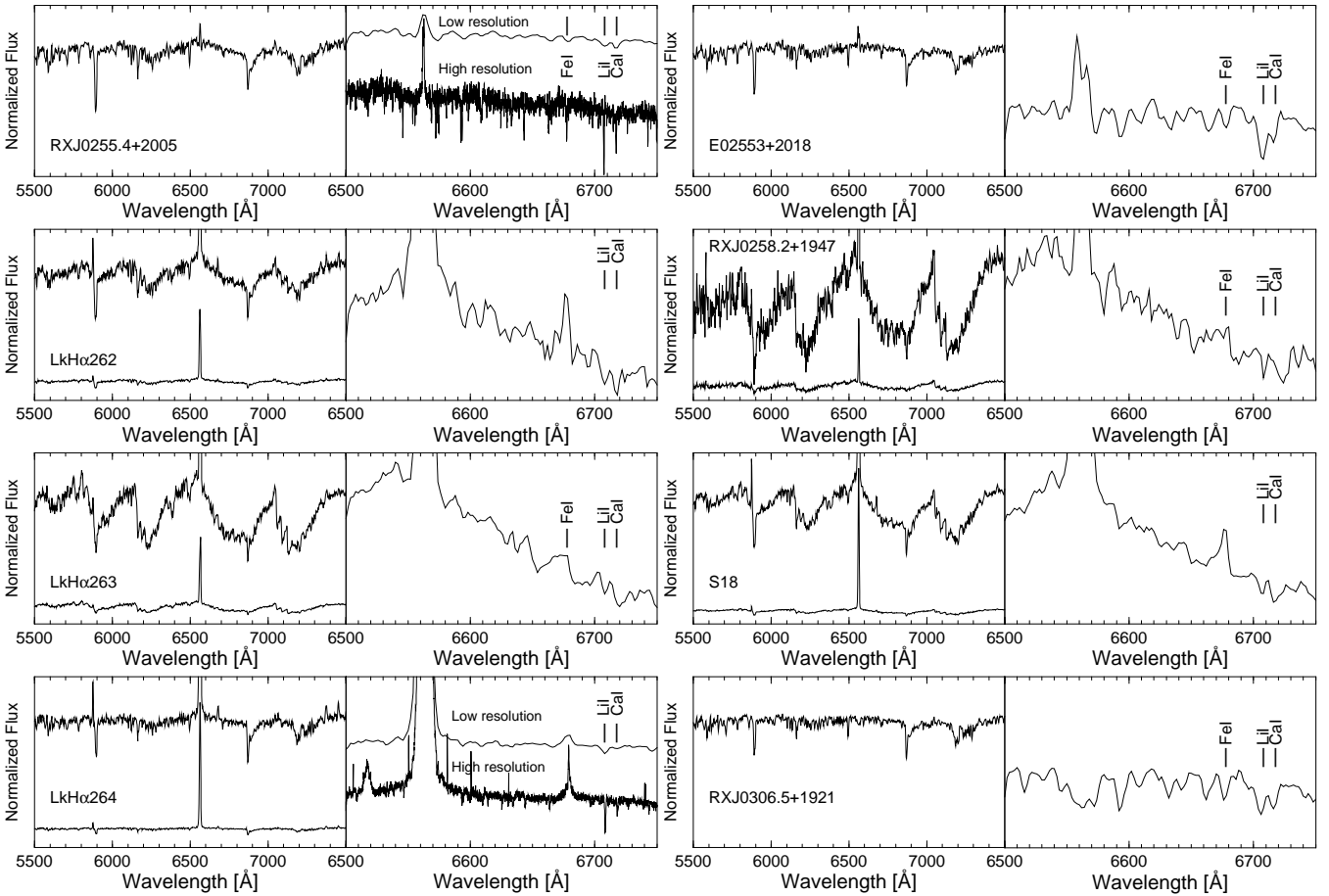
The TTS in MBM12 are clearly lithium-rich relative to the stars in the Pleiades. However, current age dependent stellar population models predict that there should be a population of young stars with ages < 150 Myr distributed across the sky. Therefore we compare the density of young X-ray sources detected in MBM12 with the age dependent stellar population model of Guillout et al. (1996) to find out if we are really seeing an excess of young X-ray sources in the direction of MBM12. In the galactic latitude range of $40^\circ > |b| > 30^\circ$ Guillout et al. (1996) predict there

⁵ Magnitudes for the sources indicated with a “:” are estimated from the digitized sky survey images

Table 5. $H\alpha$ and LiI 6708Å equivalent widths for the stars in MBM12 in which lithium was detected.

Star	RA [2000]	Dec [2000]	SpT	$\log T_{\text{eff}}$	V [mag]	$W(H\alpha)^a$ [Å]	$W(\text{Li})$ [mÅ]	$W(\text{Li})$ hi-res [mÅ]	$W(\text{Li})$ de veiled [mÅ]	$\log N(\text{Li})$
Main sequence stars										
HD 17332	02:47:27.3	+19:22:24	G1V	3.769	6.8	2.96	190	3.2
RXJ0255.3+1915	02:55:16.5	+19:15:02	F9	3.785	10.4	3.75	170	3.3
T Tauri stars										
RXJ0255.4+2005	02:55:25.7	+20:04:53	K6	3.631	12.2	-1.26	380	440 ± 10	462	2.7
LkH α 262	02:56:07.9	+20:03:25	M0	3.584	14.6	-32.1	290	...	412	2.0
LkH α 263	02:56:08.4	+20:03:39	M4	3.517	14.6	-32.9	380	...	543	1.6
LkH α 264	02:56:37.5	+20:05:38	K5	3.644	12.5	-58.9	490	510 ± 20	836	3.8
E02553+2018	02:58:11.2	+20:30:04	K4	3.657	12.3	-1.6	620	475^b	499	3.1
RXJ0258.3+1947	02:58:15.9	+19:47:17	M5	3.501	15.0	-24.5	580	...	783	1.8
S18	03:02:21.1	+17:10:35	M3	3.532	13.5	-79.0	310	...	552	1.8
RXJ0306.5+1921	03:06:33.1	+19:21:52	K1	3.698	11.4	filled	350	3.1

^a A negative sign denotes emission. ^b The high resolution measurement of $W(\text{Li})$ for this star is taken from Martín et al. (1994).

**Fig. 3.** Spectra are displayed for the 8 currently known TTS in MBM12.

should be 0.6–1.0 stars deg^{-2} and 0.14–0.20 stars deg^{-2} above an X-ray count rate threshold of 0.0013 cts s^{-1} and 0.03 cts s^{-1} , respectively, which have ages < 150 Myr. Therefore, we expect to detect ~ 1.9 –3.1 young stars in this age group in the *ROSAT* pointed observation and 3.5–5 stars in this age group in the RASS observation. Since we observed several young stars which probably have ages

< 150 Myr but are not associated with MBM12 (i.e., the two intermediate spectral type stars which have not yet depleted their lithium and the 3 Me and 3 Ke stars listed in Table 4 which have depleted their lithium but show $H\alpha$ emission), there are a sufficient number of X-ray active stars in this region to account for the numbers predicted by Guillout et al. (1996). Therefore, the TTS we observe

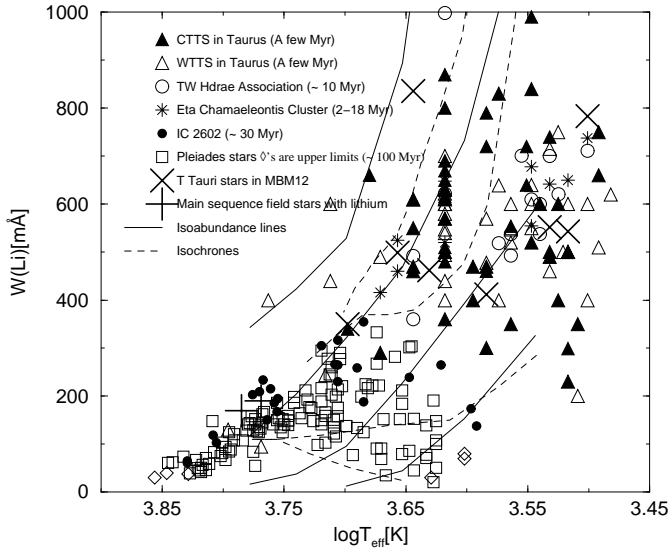


Fig. 5. The stars in which we detected lithium are displayed in an $W(\text{Li})$ v. T_{eff} diagram. For comparison, we also display stars from Taurus (\sim a few Myr; Strom et al. 1989; Basri et al. 1991; Patterer et al. 1993; Marcy et al. 1994; Martín et al. 1994), the TW Hydrae Association (\sim 10 Myr; Webb et al. 1999), the η Chamaeleontis Cluster (\sim 2–18 Myr; Mamajek et al. 1999), IC 2602 (\sim 30 Myr; Randich et al. 1997) and the Pleiades (\sim 100 Myr; Soderblom et al. 1993). The solid lines are $\log N(\text{Li}) = 4.3, 3.2, 2.1$ isoabundance lines (from top to bottom, respectively) for the non-LTE curves of growth of Pavlenko & Magazzù (1996) for $\log g = 4.5$ stars and the dashed lines are the 1, 10, 30, 100 Myr isochrones (from top to bottom, respectively) for the non-rotating lithium depletion model of Pinsonneault et al. (1990) normalized to $\log N(\text{Li}) = 3.3$ on a scale where $\log N(\text{H}) = 12$. The location of the MBM12 TTS in the diagram relative to that of the stars in the other nearby young clusters indicates they are ≤ 10 Myr.

represent an excess of X-ray active young stars associated with MBM12.

In addition to the X-ray selected T Tauri star candidates, we also observed the reddest star from a list of stars compiled by Duerr & Craine (1982b) which are along the line of sight to MBM12 and have V-I colors redder than 2.5 mag. The optical spectrum of this star, which we will call DC48, indicates it is a G9 star. Since Duerr & Craine (1982b) measured $V = 18.7$ and $V-I = 5.6$ mag, it corresponds to a main sequence star with $A_v \sim 8.9$ mag at a distance of ~ 63 pc or a giant star with $A_v \sim 8.4$ mag at a distance of ~ 950 pc. The spectrum of the highly reddened ($A_v \sim 8.4$ – 8.9) G9 star, DC48, is displayed in Fig. 4.

5. X-ray variability of the TTS

We tested all of the TTS for X-ray variability using the methods described in Hambaryan et al. (1999). The only

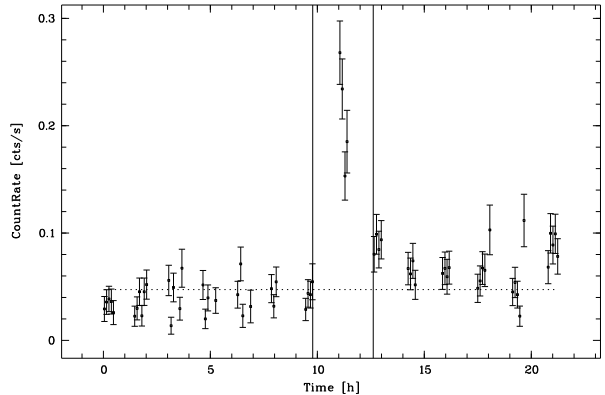


Fig. 6. An X-ray light curve is displayed for the star, RXJ0255.4+2005, that was found to flare during the *ROSAT* pointed observation. The ~ 25 ks exposure of the star is displayed in 400 second bins. The vertical lines mark the divisions between the pre-flare, flare, and post-flare phases used for the X-ray spectral fits.

T Tauri Star which showed X-ray variability is the newly identified star RXJ0255.5+2005 that was detected both in the RASS and in the *ROSAT* pointed observation and flared during the pointed observation (see the light curve displayed in Fig. 6). The peak X-ray count rate during the flare increased by more than a factor of 6 from the pre-flare count rate. Although we do not have a sufficient number of counts (~ 1000 counts for the non-flare phase and ~ 500 counts for the flare phase) for a detailed study of the evolution of the coronal temperature during the flare, we performed a rough spectral fit using a 2 temperature Raymond-Smith model (Raymond & Smith 1977) including a photoelectric absorption term using the Morrison & McCammon (1983) cross sections. We fit the data for 3 time intervals: the pre-flare phase, the flare, and the post-flare phase Fig. 7. Both temperature components increased during the flare and remained high throughout the post-flare phase. The parameters derived from the X-ray spectral fits are listed in Table 6 (see Sect. 6 for a description of the Table columns). Since the two temperature components are not well constrained by the spectral fit during the flare, these estimates should be viewed as a lower limits. The results of the spectral fits are consistent with the type of coronal heating seen in high signal-to-noise X-ray spectra of other flaring WTTS (e.g., Tsuboi et al. 1998).

6. The X-ray luminosity function

Although our X-ray spectra do not have sufficiently high signal-to-noise for a detailed comparison of X-ray spectral models, we performed a spectral fit using a 2 temperature Raymond-Smith model including a photoelectric absorption term as described in Sect. 5 for the sources

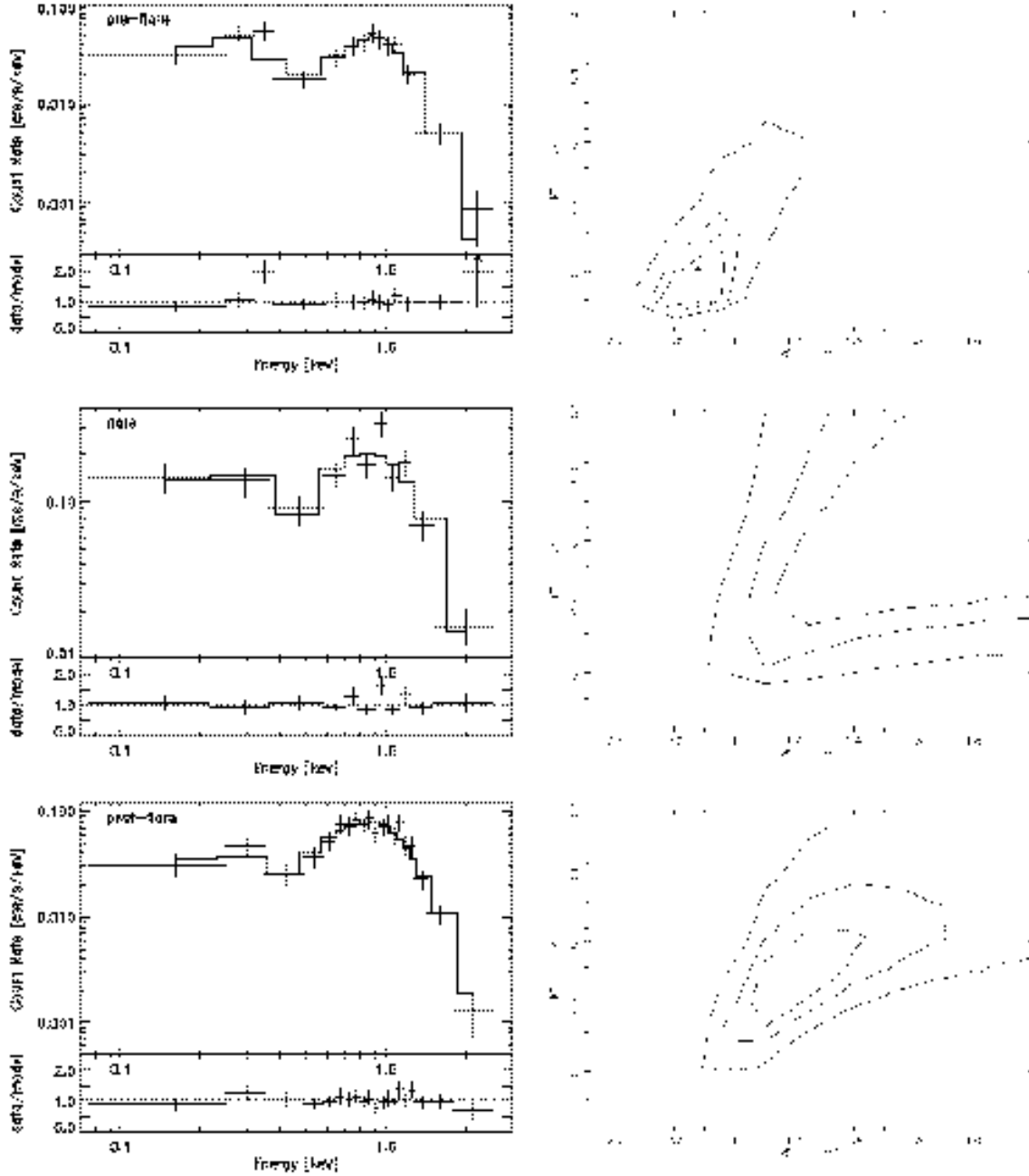


Fig. 7. The X-ray spectra and the best-fit 2 temperature Raymond-Smith model are displayed for the pre-flare, flare, and post-flare phases of the *ROSAT* PSPC observation of the weak-line T Tauri star RXJ0255.4+2005. The corresponding χ^2 plots indicate that both temperature components increased during the flare.

with at least 100 counts. For the sources with fewer than 100 counts we calculate the X-ray flux using an X-ray count rate to flux conversion factor of 1.1×10^{-11} erg cts $^{-1}$ cm $^{-2}$ which is the mean conversion factor derived from the spectra for which we performed spectral fits. We list the total *ROSAT* broad band (0.08–2.0 keV)

counts and count rates for the TTS in MBM12 and the derived interstellar+circumstellar absorption cross sections and plasma temperatures for the spectra in which we performed spectral fits in Table 6. The X-ray luminosities assume a distance of 65 pc. Since the binary LkH α 262/263 was not spatially resolved with the PSPC we fit the com-

bined X-ray spectrum to estimate the combined X-ray luminosity but we divide that value in half to generate the X-ray luminosity function.

In order to compare the derived X-ray luminosity function for the TTS in MBM12 with other flux limited X-ray luminosity functions we used the ASURV Rev. 1.2 package (Isobe & Feigelson 1990; LaValley et al. 1992), which implements the methods presented in Feigelson & Nelson (1985). Although the currently known TTS in MBM12 are all X-ray detected, the luminosity functions of other, more distant, star forming regions include upper limits. The derived X-ray luminosity function is displayed in Fig. 8 with the X-ray luminosity function for the TTS in the L1495E cloud in Taurus which (like MBM12) was observed in a deep (33 ks) *ROSAT* PSPC pointed observation (Strom & Strom 1994). The *ROSAT* pointed observation of L1495E is ~ 20 times more sensitive than previous observations with the *Einstein* satellite. Strom & Strom (1994) used this observation to show that the X-ray luminosity of TTS extends to fainter luminosities than were observed with *Einstein*. We have re-reduced the pointed observation of L1495E in a way analogous to that of MBM12. The X-ray luminosity function we derive for L1495E (1) includes only the K and M spectral type TTS, (2) includes 6 upper limits, (3) assumes an X-ray to optical flux conversion factor of 1.1×10^{-11} erg cts $^{-1}$ cm $^{-2}$, and (4) assumes a distance of 140 pc. The X-ray luminosity functions in MBM12 and L1495E agree well: in MBM12 the $\log L_{\text{x, mean}} = 29.0 \pm 0.1$ erg s $^{-1}$ and $\log L_{\text{x, median}} = 28.7$ erg s $^{-1}$; in L1495E $\log L_{\text{x, mean}} = 28.9 \pm 0.2$ erg s $^{-1}$ and $\log L_{\text{x, median}} = 28.9$ erg s $^{-1}$. However, we note that the MBM12 X-ray luminosity function has a lower high-luminosity limit and a higher low-luminosity limit than the L1495E X-ray luminosity function. Therefore, although the pointed observation of MBM12 is more sensitive than the pointed observation L1495E (because MBM12 is much closer) our follow-up observations of the TTS in MBM12 may be incomplete for sources fainter than $V \sim 15.5$ mag. In addition, since we know that one of our X-ray sources, S18, is detected but below our threshold for follow-up observations, there may be other, fainter, X-ray emitting TTS in MBM12 with spectral types later than $\sim M2$ (i.e., the spectral type of S18) that will be discovered in more sensitive follow-up observations. The discrepancy at the high luminosity end of the X-ray luminosity function may also be explained if the distance to the TTS in MBM12 is larger than 65 pc. Although an increased distance is allowed by the recent *Hipparcos* results it should be confirmed with further observations.

7. Conclusions

Although MBM12 is not a prolific star-forming cloud when compared to nearby giant molecular clouds it is the nearest star-forming cloud to the sun and offers a unique opportunity to study the star-formation process within a

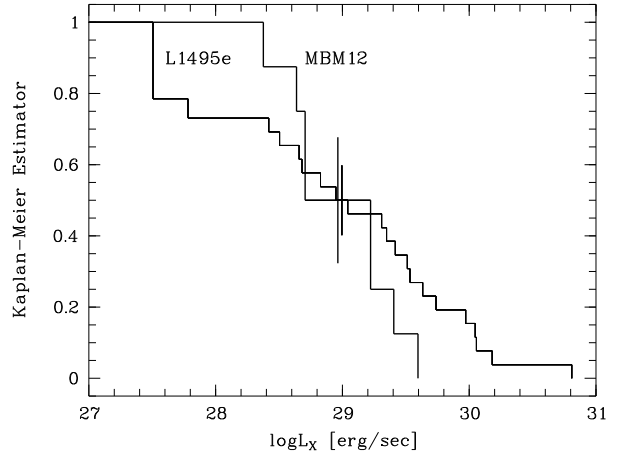


Fig. 8. The X-ray luminosity function for the TTS in MBM12 is displayed with a similar X-ray luminosity function for the TTS in the L1495E cloud in Taurus. Distances of 65 pc and 140 pc are assumed for the X-ray luminosity functions of MBM12 and L1495E, respectively. The error bars shown are the largest for each data set.

molecular cloud at high sensitivity. We have presented follow-up observations of X-ray stars identified in the region of the MBM12 complex. These observations have doubled the number of confirmed TTS in this region. Since the *ROSAT* PSPC pointed observation of the central region of the cloud was sensitive enough to detect all of the previously known TTS in the cloud, we believe the list of 5 CTTS and 3 WTTS presented in Table 5 to be a nearly complete census of the TTS in MBM12 for spectral types earlier than $\sim M2$. Assuming a mean mass of $\sim 0.6 M_{\odot}$ for the 8 currently known TTS in MBM12 and a cloud mass of 30–200 M_{\odot} (Pound et al. 1990; Zimmermann & Ungerechts 1990) the star-formation efficiency of MBM12 is ~ 2 –24%. Since the currently known TTS population in MBM12 is incomplete only for the lower mass objects, unless there are a huge number of these objects yet to be discovered in the cloud, this estimate of the star-formation efficiency will not change significantly. Although there is still a large uncertainty in the mass of the cloud the estimated star-formation efficiencies are consistent with that expected from clouds with masses on the order of 100 M_{\odot} (Elmegreen & Efremov 1997). By comparing the strengths of the $H\alpha$ emission and Li I $\lambda 6708$ Å absorption lines of the TTS in MBM12 with those found in other young clusters, we place an upper limit on the age of the stars in MBM12 ~ 10 Myr.

By comparing the X-ray luminosity function of the TTS in MBM12 with that of the TTS in L1495E we predict that there are more young, low-mass, stars to be discovered in MBM12 and the assumed distance to the cloud may have to be increased. Although this prediction agrees

Table 6. X-ray parameters in the 0.08–2.0 keV band for the TTS in MBM12

Star	RASS		Pointed Obs.		$N_{\text{H}}/10^{21}$ [cm^{-2}]	kT_{high} [keV]	kT_{low} [keV]	χ^2/dof	$f_{\text{x}}/10^{-13}$ [$\text{erg s}^{-1} \text{cm}^{-2}$]	$\log L_{\text{x}}$ [erg s^{-1}]
	Counts	Rate [cts s^{-1}]	Counts	Rate [cts s^{-1}]						
RXJ0255.4+2005										
“ ” total	17 ± 5	0.04 ± 0.01	1719 ± 52	0.067 ± 0.002	0.86	0.89	0.08	39.7/34	7.81	29.60
“ ” pre-flare	524 ± 29	0.043 ± 0.002	0.49	0.88	0.11	9.2/9	4.12	29.32
“ ” flare	368 ± 22	0.22 ± 0.01	0.18	1.69	0.30	9.5/6	20.1	30.01
“ ” post-flare	781 ± 35	0.071 ± 0.003	0.27	1.14	0.24	10.7/15	6.96	29.55
LkH α 262/263	340 ± 21	0.016 ± 0.001	2.65	0.97	0.16	6.29/8	2.01	29.01
LkH α 264	89 ± 12	0.0043 ± 0.0006	0.47	28.39
E02553+2018	9 ± 4	0.04 ± 0.02	575 ± 34	0.036 ± 0.002	8.21	1.05	0.10	16.5/16	5.03	29.41
RXJ0258.3+1947	182 ± 16	0.0079 ± 0.0007	8.42	1.14	0.13	2.63/2	0.86	28.64
S18	6 ± 3	0.03 ± 0.01	3.30	29.22
RXJ0306.5+1921	12 ± 4	0.03 ± 0.01	3.30	29.22

with the recently revised distance estimate to the cloud ($\sim 65 \pm 35$ pc) based on results of the *Hipparcos* satellite, it should be confirmed with future observations.

We have also identified a reddened G9 star behind the cloud with $A_{\text{v}} \sim 8.4$ –8.9 mag. Therefore, there are at least two lines of sight through the cloud that show larger extinctions ($A_{\text{v}} > 5$ mag) than previously thought for this cloud. This higher extinction explains why MBM12 is capable of star-formation while most other high-latitude cloud are not.

Acknowledgements. We wish to thank Patrick Guillout for helpful discussions about the expected population of young X-ray active stars located at high galactic latitude and Loris Magnani for insightful comments concerning this paper. We also thank an anonymous referee for suggestions which enable us to put firmer constraints on the age of the TTS in MBM12. The *ROSAT* project is supported by the Max-Planck-Gesellschaft and Germany’s federal government (BMBF/DLR). TH is grateful for a stipendium from the Max-Planck-Gesellschaft for support of this research. RN acknowledges a grant from the Deutsche Forschungsgemeinschaft (DFG Schwerpunktprogramm “Physics of star formation”)

References

Ballesteros-Paredes J., Hartmann L., Vázquez-Semadeni E., 1999, *ApJ*, in press
 Basri G., Martín E.L., Bertout C., 1991, *A&A* 252, 625
 Bhatt H. C., Jain S. K., 1992, *A&A* 257, 57
 Briel U.G., Pfeiffermann E., 1995, in *Proc. SPIE Vol. 2518, EUV, X-ray, & Gamma-Ray Instrumentation for Astronomy VI*, eds. O.H. Siegmund, J.V. Vallerga, 120
 Caillaud J.-P., Magnani L., Fryer C., 1995, *ApJ* 441, 261
 Covino E., Alcalá J.M., Allain S., et al. 1997, *A&A* 328, 187
 Damiani F., Micela G., Sciortino S., Harnden F.R., Jr., 1995, *ApJ* 446, 331
 de Jager C., Nieuwenhuijzen H., 1987, *ApJ* 177, 217
 Downes R.A., Keyes C.D., 1988, *AJ* 96, 1988
 Duerr R., Craine E.R., 1982a, *AJ* 87, 408
 Duerr R., Craine E.R., 1982b, *PASP* 94, 567
 Elmegreen B.G., 1993, in *Protostars and Planets III*, eds. E. Levy, J. Lunine (University of Arizona Press), 97

Elmegreen B.G., Efremov Y.N., 1997, *ApJ* 480, 235
 Feigelson E., 1996, *ApJ* 468, 306
 Feigelson E., Nelson P.I., 1985, *ApJ* 293, 192
 Fernández M., Ortiz E., Eiroa C., Miranda L.F., 1995, *A&AS* 114, 439
 Gameiro J.F., Lagor M.T.V., Lima N.M., Cameron A.C., 1993, *MNRAS* 261, 11
 Gioia M., Maccacaro T., Schild R.E., et al., 1990, *ApJS* 72, 567
 Guillout P., Haywood M., Motch C., Robin A.C., 1996, *A&A* 316, 89
 Hambaryan V., Neuhäuser R., Stelzer B., 1999, *A&A* 345, 121
 Hearty T., Magnani L., Caillaud J.-P., et al., 1999, *A&A* 341, 163
 Herbig G.H., 1977, *ApJ* 214, 747
 Herbig G.H., Bell K.R., 1988, *Lick Observatory Bulletin* 1111, 1
 Hobbs L.M., Blitz L., Magnani L., 1986, *ApJ* 306, L109
 Hobbs L.M., Blitz L., Penprase B.E., Magnani L., Welty D.E., 1988, *ApJ* 327, 356
 Isobe T., Feigelson E., 1990, *BAAS* 22, 917
 Kastner J.H., Zuckerman B., Weintraub D.A., Forveille T., 1997, *Science* 277, 67
 LaValley M., Isobe T., Feigelson E., 1992, *BAAS* 1, 245
 Lépine J.R.D., Duvert G., 1994, *A&A* 286, 60
 Lynds B.T., 1962, *ApJS* 7, 1
 Magnani L., Blitz L., Mundy L., 1985, *ApJ* 295, 402
 Magnani L., Caillaud J.-P., Buchalter A., Beichman C.A., 1995, *ApJS* 96, 159
 Mamajek E., Lawson W.A., Feigelson E.D., 1999, *ApJ* 516, 77
 Marcy G.W., Basri G., Graham J.R., 1994, *ApJ* 428, L57
 Martín E.L., Rebolo R., Magazzù A., Pavlenko Ya.V. 1994, *A&A* 282, 503
 Moriarty-Schieven G.H., Andersson B.-G., Wannier P.G., 1997, *ApJ* 475, 642
 Morrison R., McCammon, D. 1983, *ApJ* 270, 119
 Neuhäuser R., Sterzik M.F., Schmitt J.H.M.M., Wichmann R., Krautter J., 1995, *A&A* 297, 391
 Patterer R.J., Ramsey L., Huenemoerder D.P., Welty A.D., 1993, *AJ* 105, 1519
 Pavlenko Ya. V., Magazzù A., 1996, *A&A* 311, 961
 Pinsonneault M. H., Kawaler S. D., Demarque P., 1990, *ApJ* 74, 501

- Pound M.W., Bania T.M., Wilson R.W., 1990, ApJ 351, 165
Queloz D., 1994, in IAU symposium 167, Ed. A.G. Davis Philip,
p. 221
Randich S., Aharpour N., Pallavicini R., Prosser C. F., Stauffer
J. R., 1997, A&A 323, 86
Raymond J.C., Smith B.W., 1977, ApJS 35, 419
Soderblom D., Pendelton J., Pallavicini R., 1989, AJ 97, 539
Soderblom D.R., Jones B.F., Balachandran S., et al., 1993, AJ
106, 1059
et al., 1994, ApJS 91, 625
Stephenson C.B., 1986, ApJ 300, 779
Sterzik M.F., Durisen R., 1995, A&A 304, L9
Stocke J.T., Morris S.L., Gioia I.M., et al., 1991, ApJS 76, 813
Strom K.M., Strom S.E., 1994, ApJ 424, 237
Strom K., Wilkin F., Strom S., Seaman R., 1989, AJ 98, 1444
Trümper J., 1983, Adv. Space Res. 2, 241
Tsuboi Y., Koyama K., Murakami H., et al., 1998, ApJ 503,
894
Webb R. A., Zuckerman B., Platais I., et al., 1999, ApJ 512,
L63
Zimmermann T., Ungerechts H., 1990, A&A 238, 337
Zuckerman B., Becklin E.E., McLean I.S., Patterson J., 1992,
ApJ 400, 665